Preparation and Properties of Holocellulose Nanofibrils with Different Hemicellulose Content

Chan-Woo Park,[a] Song-Yi Han,[a] Seon-Kang Choi,[b] and Seung-Hwan Lee [a,*]

The hemicellulose content in holocellulose was adjusted by an alkaline treatment. The effects of this treatment on the defibrillation efficiency of holocellulose nanofibrils (HCNFs) were investigated by wet disk-milling (WDM), along with their morphological and physical properties. In addition, the tensile properties of nanopaper sheets fabricated with these HCNFs were investigated. As the hemicellulose content decreased, the average diameter and the filtration time of the HCNFs decreased, whereas specific surface area and crystallinity index increased. An increase in the WDM time reduced the average diameter and crystallinity of the HCNFs and increased their filtration time and specific surface area. The tensile strength and elastic modulus of the nanopaper sheets increased with increased hemicellulose content and WMD time.

INTRODUCTION

Cellulose is the most abundant, renewable natural biopolymer on earth. It is generally obtained from woody biomass *via* photosynthesis – a process that produces approximately tens of billions of tons of cellulose annually (Cheng *et al.* 2007; Habibi *et al.* 2010). In the wood cell wall, cellulose molecules form microfibrils *via* intra- or intermolecular hydrogen bonds (Aulin *et al.* 2011). The cellulose microfibril has a diameter of 10 nm to 30 nm and can be isolated after chemical or biological pretreatments through mechanical defibrillation processes, such as wet disk-milling (WDM), high-pressure homogenizing, and ball milling (Habibi *et al.* 2010; Siró and Plackett 2010; Wang *et al.* 2012; Espinosa *et al.* 2013; Jang *et al.* 2013; Peng *et al.* 2013; Yu *et al.* 2013; Zhang *et al.* 2015). However, it is difficult to degrade the wood cell wall into its constituents because of its structural heterogeneity and complexity, endowing it with very strong recalcitrant characteristics against chemical or biological treatments (Himmel *et al.* 2007). Therefore, it is indispensable to pretreat lignocellulosic biomass before the defibrillation process to overcome its recalcitrance (Chang *et al.* 2012; Jang *et al.* 2013). The main role of the pretreatment is to effectively disturb the tightened structure of lignocellulosic biomass by removing hemicellulose and lignin (Lee *et al.* 2010; Siró and Plackett 2010). To this end, various pretreatment methods for the improvement of the defibrillation process have been reported, such as alkaline, enzyme, hot-compressed water (HCW), ozone, and steam explosion treatments, *etc*. However, it is not always necessary for these pretreatments to completely remove the hemicellulose and lignin (Iwamoto *et al.* 2008; Lee *et al.* 2010; Abraham *et al.* 2011; Jang *et al.* 2013). The partial removal of hemicellulose and lignin can

improve defibrillation, and the resulting product has a different chemical composition, which will influence the properties of the fibrillated products. Jang *et al.* (2013) reported that the partial removal of lignin and hemicellulose by ozone and steam treatments improved the efficiency of defibrillation. Iwamoto *et al.* (2008) reported that the amount of hemicellulose in pulp affects the ease of defibrillation and the properties of the produced paper sheets. Galland *et al.* (2015) prepared holocellulose nanofibers (HCNFs) using the acid chlorite method for delignification, reporting that the content of hemicellulose in HCNF influenced the properties of the nanopaper sheets. The obtained HCNFs are unique in terms of their high molecular weight and cellulose-hemicellulose core-shell structure. This structure can also be designed by coating hemicellulose on a pure cellulose nanofiber surface, resulting in the improvement of the hygromechanical properties and moisture stability (Prakobna *et al.* 2015a,b).

In this study, the hemicellulose content in HCNF was adjusted by an alkali treatment, and its effect on the defibrillation efficiency, morphological, and crystalline properties of HCNF was investigated. Furthermore, the tensile properties of HCNF nanopaper sheets were also investigated.

EXPERIMENTAL

Materials

A Korean white pine (*Pinus koraiensis* Sieb. et Zucc.) sample was obtained from Kangwon National University's Experimental Forest, and it was cutter-milled to 0.45 mm. Sodium chlorite ($NaClO_2$), acetic acid (CH_3COOH), and sodium hydroxide (NaOH) were purchased from Daejung Chemical & Materials Co. (Siheung, Republic of Korea). Other chemicals were purchased from commercial sources and used without further purification.

Delignification and alkaline treatment

Delignification was performed by following the Wise method (Wise *et al*. 1946). First, wood powder (20 g) and distilled water (1,200 mL) were poured into a round flask (2-L), and they were kept in a water bath at 80 °C for 20 min under constant stirring at 150 rpm. The delignification reaction was initiated by adding sodium chlorite (8 g) and acetic acid (1600 µL) into the suspension, which was continuously stirred for 1 h. The same amount of sodium chlorite and acetic acid were added every hour, and the process was repeated 7 times. The residue, holocellulose, was then vacuum-filtrated and washed with distilled water several times until the pH was neutralized.

The hemicellulose content in holocellulose was adjusted *via* an alkaline treatment. First, 30 g of holocellulose were poured into 1%, 3%, and 5% sodium hydroxide solutions (750 mL), and the reaction was performed at 25 °C for 24 h under constant stirring at 150 rpm. Next, the reactant was further reacted at 80 °C for 2 h to extract the hemicellulose, according to Abe *et al.* (2007). At the end of the reaction, a 10% acetic acid solution (750 mL) was added into the reactant for neutralization. Then, the insoluble residue was vacuum filtrated and washed with distilled water several times. The content of hemicellulose was calculated by subtracting the weight of the pure cellulose obtained by using a 17.5% NaOH treatment on the holocellulose. The sample codes and composition of cellulose and hemicellulose are summarized in Table 1.

Table 1. Sample Codes and Chemical Composition of Holocellulose

Sample Code	Concentration of NaOH solution (%)	Cellulose (%)	Hemicellulose (%)
HCNF-23	1.0	77.4	22.6
HCNF-14	3.0	87.4	13.6
HCNF-9	5.0	90.8	9.2

Preparation of HCNF

The holocellulose was suspended to a 1.0 wt.% concentration (1500 mL), and then subjected to WDM (Supermasscolloider, MKCA6-2, Masuko Sangyo Co. Ltd., Kawaguchi, Japan). The rotational speed was set at 1,800 rpm, and the clearance between the upper and lower disks was reduced to between 100 µm and 150 µm from the zero point, at which distance the disks would begin to rub. The operation was repeated until the fifth pass.

Methods

Morphology

The HCNF suspensions were diluted to 0.001 wt.% and then sonicated using an ultrasonicator (VCX130PB, Sonics & Materials Inc., Newtown, USA) for 1 min. The suspensions were vacuum-filtrated on a polytetrafluoroethylene (PTFE) membrane filter with a pore size of 0.2 µm (ADVANTEC®, Toyo Roshi Kaisha Ltd., Tokyo, Japan). The filtrated products were stacked on the PTFE filter and immersed in tert-butyl alcohol for 30 min. This procedure was repeated thrice to completely exchange the water with tert-butyl alcohol. The HCNFs were freeze-dried using a freeze dryer (FDB-5502, Operon Co. Ltd., Gimpo, Korea) at -55 °C for 3 h to prevent the aggregation of HCNFs. The freeze-dried samples were coated with carbon using a vacuum evaporator (JEE-400, JEOL Ltd., Tokyo, Japan) with an electric current of 30 mA. The morphologies of the HCNFs were observed with a scanning electron microscope (SEM, S-4800, Hitachi Ltd., Tokyo, Japan) in the Central Laboratory of Kangwon National University. The diameter of the individual fibers was measured at least 800 times for each sample by an open-sourced Image J program (1.45 ver. for Windows, National Institute of Mental Health [NIMH] of the National Institute of Health [NIH], Bethesda, USA).

Specific surface area (SSA)

The HCNF suspensions (30 mL) were centrifuged (VS-21SMTi, Vision Scientific Co. Ltd., Bucheon, Republic of Korea) at 20,000 rpm for 15min, and the supernatant was drained. Then, tert-butyl alcohol was poured into the centrifuge tube, and it was mixed with the centrifuged HCNFs using a vortex mixer (IKA® MS2 mini shaker, IKA Werke, Germany). This solvent exchange was repeated 15 times to completely exchange the water with tert-butyl alcohol and prevent the aggregation of HCNFs. The solvent exchanged HCNFs were freeze-dried with powder at -55 °C for 12 h. The specific surface area of the HCNFs was measured using a sorption analyzer (BELSORP-Max, BEL Japan Inc., Toyonaka, Japan) by N_2 adsorption at 77 K.

Crystallinity index and average crystallite size

The x-ray diffraction profiles of the HCNFs were detected using a diffractometer (RINT TTR III, Rigaku Co. Ltd., Tokyo, Japan) with Cu-Kα radiation (K = 0.15418 nm).

The samples were scanned in 2θ ranges varying from 0° to 40° at a 2°/min scanning rate. The crystallinity index and average crystallite size of the HCNFs were calculated from the x-ray diffraction profiles following Eq. 1 (Segal *et al.* 1959) and Eq. 2 (Monshi *et al.* 2012), respectively,

$$Crystallinity\ Index\ (\%)\ =\ \frac{I_{200} - I_{amor}}{I_{200}} \times 100$$

(1)

where I_{200} is the maximum intensity of the peak from the (200) lattice plane ($2\theta = 22.5°$), and I_{amor} is the peak intensity of the amorphous phases ($2\theta = 18.5°$). Equation 2 is listed as,

$$Average\ crystallite\ size\ (nm)\ =\ \frac{K\lambda}{\beta cos\theta}$$

(2)

where K is the Scherrer constant (0.89), λ is the wavelength of the X-ray (0.15418 nm), β is the width of the half-height of the peak angle at the (200) plane in radians, and θ is the Bragg angle corresponding to the (200) plane.

Nanopaper preparation and tensile testing

First, 0.2 wt.% HCNF suspensions (220 mL) were prepared, sonicated for 1 min, and vacuum-filtrated on a silicone-coated filter (Whatman® No. 2200 125, GE Healthcare Ltd., Buckinghamshire, UK). At this stage, the filtration time was measured as a criterion of the degree of fibrillation. The filtrated HCNFs were sandwiched between the silicone-coated filters and pressed at 105 °C with a pressure of 5 MPa for 2 min using a hot press.

For the tensile test, 7 specimens with dimensions of 5.0 mm × 0.7 - 0.8 mm × 50.0 mm (width × thickness × length) were cut from the nanopaper and kept in a thermo-hygrostat at 25 °C and 50% relative humidity to minimize the effect of the relative humidity on the tensile properties of the nanopaper sheets. The tensile test was conducted using a testing machine (H50K, Hounsfield Test Equipment Ltd., Redhill, UK), at a cross-head speed of 10 mm/min, with a specimen span length of 30 mm.

RESULTS AND DISCUSSION

Morphological Properties

As shown in Table 1 of the Experimental section, the content of hemicellulose in holocellulose was successfully adjusted by changing the concentration of the NaOH solution, in which a range of hemicellulose of 9.2 wt.% to 22.6 wt.% was obtained. The effects of the hemicellulose content and the number of WDM passes on the morphological properties of the HCNFs were investigated. Figure 1 shows the SEM images of various HCNFs. All of the samples showed a fine and uniform morphology, and a decreased diameter was observed as the hemicellulose content decreased, and the number of WDM passes increased.

Table 2 and Fig. 2 summarize the average diameter and distribution of HCNFs with different hemicellulose content and number of WDM passes, respectively. The average diameter of the HCNFs decreased as the hemicellulose content decreased, as shown in Table 2. Holocellulose has a core-shell structure, *i.e.*, hemicellulose covered cellulose, thus the diameter of HCNF may be subject to the amount of hemicellulose. The average diameter decreased for all of the samples as the number of WDM passes increased.
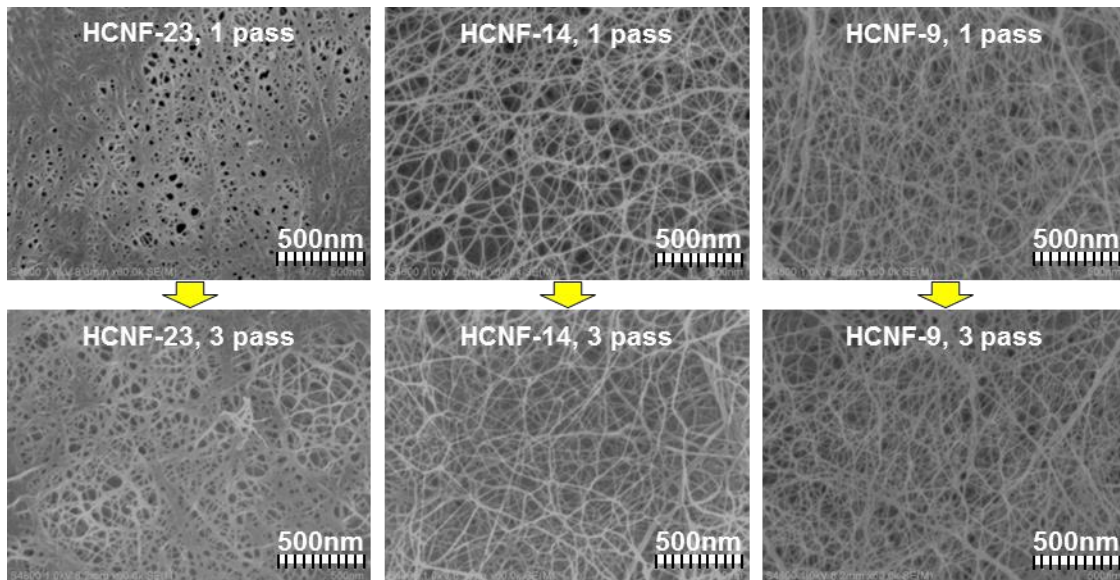
bioresources.com

Fig. 1. SEM images of HCNFs with different hemicellulose content and number of WDM passes

As shown in Fig. 2, the distribution of the diameters became narrow as the content of hemicellulose decreased in both cases of 1 and 3 WDM passes. All HCNFs showed a diameter of less than 55 nm. The diameter distribution peak shifted to a smaller size with an increased number of WDM passes. Iwamoto *et al.* (2008) reported that holocellulose prepared by delignification using the Wise method, and pure cellulose prepared using a 6% potassium hydrate solution after delignification from Sitka spruce, were fibrillated uniformly *via* WDM into diameters of 10 nm to 20 nm. Nobuta *et al.* (2016) removed lignin and hemicellulose from kenaf bast fiber using the Wise method and an alkaline treatment using a 4% KOH solution, respectively, and prepared HCNF and pure cellulose nanofibrils (PCNF) by WDM. The diameters of HCNF and PCNF were reported to be 18 nm and 17 nm, respectively. Their results were similar to those obtained in this study.
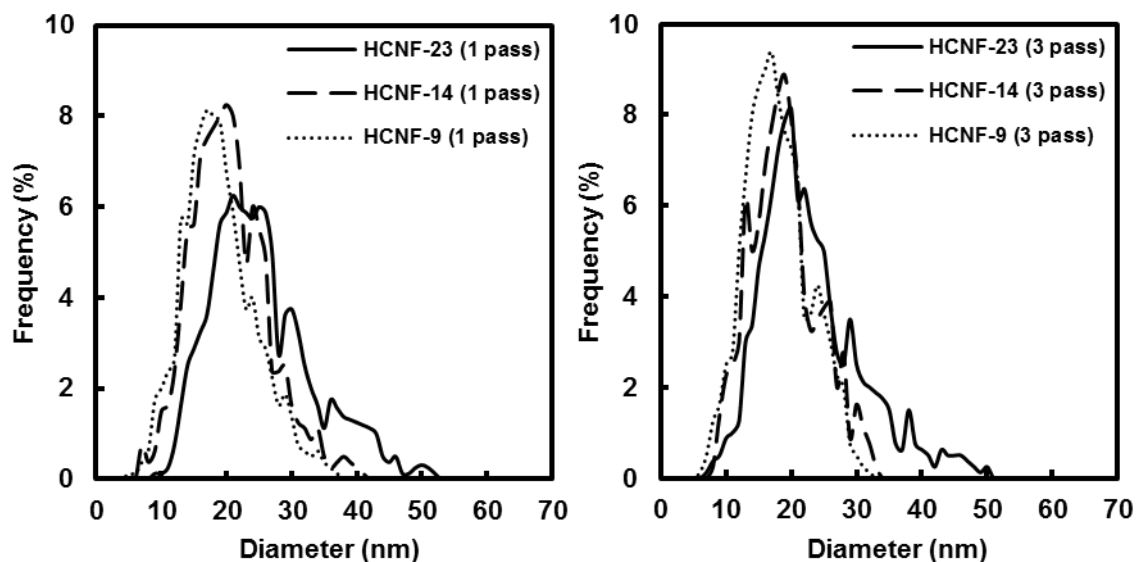

Fig. 2. Diameter distribution of HCNFs with different hemicellulose content and number of WDM passes; Note: the class intervals of the diameter distribution were 1 nm

Table 2. Average Diameter of HCNFs with Different Number of WDM Passes

Sample Code	Number of WDM Passes	Average Diameter (nm)
HCNF-23	1	25.3 ± 8.2
	3	23.1 ± 7.8
HCNF-14	1	18.6 ± 5.7
	3	17.9 ± 5.6
HCNF-9	1	18.5 ± 5.7
	3	17.9 ± 4.2

Specific Surface Area and Filtration Time

Table 3 shows the effect of the hemicellulose content and number of WDM passes on the specific surface area and filtration time of HCNFs. The specific surface area showed an increasing tendency as the hemicellulose content and number of WDM passes decreased and increased, respectively. This result corresponded well with the tendency of the HCNF diameter to decrease with decreased hemicellulose content and increased number of WDM passes. Moreover, these results supported that the removal of hemicellulose improved the defibrillation efficiency. The filtration time of the HCNF suspensions was shortened as the hemicellulose content decreased, despite their increased specific surface area. This may have been due to the strong hydrophilicity of hemicellulose. Kim *et al.* (2017) investigated filtration time of HCNF and BKP-NF (bleached kraft pulp-based nanofibril) suspensions, and the filtration time of HCNF suspensions was noticeably longer than that of the BKP-NF suspension. Iwamoto *et al.* (2008) reported that a KOH treatment to remove hemicellulose in holocellulose reduced the water retention value of HCNFs due to the reduction of hydrophilic amorphous hemicellulose substances. Pejic *et al.* (2008) reported that the water retention value of hemp fibers decreased due to the removal of hemicellulose. Similar to the specific surface area, the filtration time increased with an increased number of WDM passes.

Table 3. Specific Surface Area and Filtration Time of HCNFs with Different Hemicellulose Content Obtained by Different Number of WDM Passes

Sample code	Number of WDM Passes	Specific Surface Area (m^2/g)	Filtration Time (h)
HCNF-23	1	138	13.1
	3	170	14.5
HCNF-14	1	141	12.1
	3	177	14.2
HCNF-9	1	144	11.2
	3	175	13.0

Crystallinity Index and Average Crystallite Size

Figure 3 shows the effects of hemicellulose content and the number of WDM passes on the X-ray diffraction pattern. All of the samples showed a typical cellulose I pattern, but the peak at 22.5° (2θ) became larger with decreased hemicellulose content. Table 4 summarizes the crystallinity index and average crystallite size of the various HCNFs. As the hemicellulose content decreased, the crystallinity index increased when 1 and 3 WDM passes were performed. Wan *et al.* (2010) reported that the crystallinity index of eucalyptus

bioresources.com

kraft pulps increased as the amount of hemicellulose decreased. The increase of the crystallinity index may have been due to the removal of amorphous hemicellulose. The crystallinity index was also influenced by the number of WDM passes. With an increased number of WDM passes, the crystallinity index of all HCNFs decreased. It is thought that the crystalline structure of cellulose collapses by shear and impact forces during the WDM process. Iwamoto *et al.* (2007) also reported a decreasing tendency of crystallinity with an increasing number of WDM passes. Yu and Wu (2011) investigated the effect of ball-milling on the crystallinity of microcrystalline cellulose and reported that crystalline structures can be destroyed by severe ball-milling treatments. In all of the samples, the average crystallite size fell within the range of 3.2 nm to 3.6 nm. With decreased hemicellulose content, the average crystallite size was slightly increased. In contrast, a decreasing tendency of the average crystallite size was found with an increased number of WDM passes. Wan *et al.* (2010) also reported that the average width of cellulose crystallite increased from 4.3 nm to 4.6 nm as the hemicellulose content decreased from 27.62% to 9.09%.
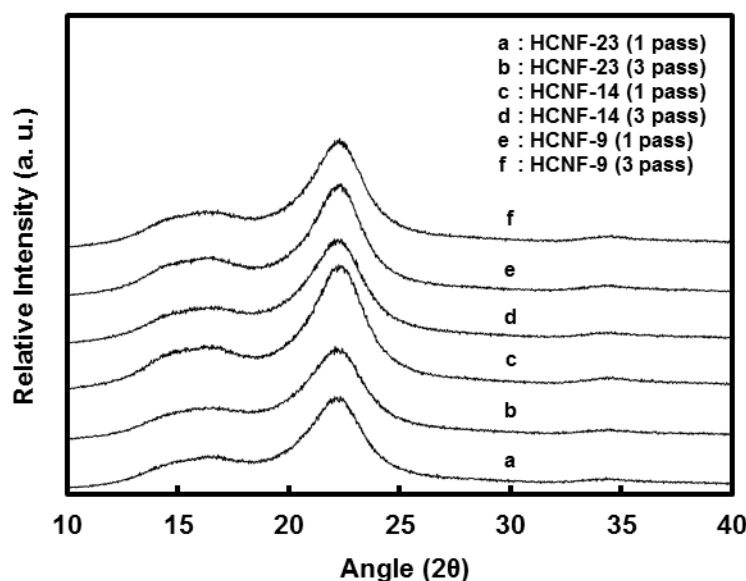

Fig. 3. X-ray diffraction spectra of HCNFs with varying hemicellulose content obtained using a different number of WDM passes

Table 4. Crystallinity Index and Average Crystallite Size of HCNFs with Different Hemicellulose Content Obtained Using a Different Number of WDM Passes

Sample Code	Number of WDM Passes	Crystallinity Index (%)	Average Crystallite Size (nm)
HCNF-23	1	69	3.2
	3	67	3.2
HCNF-14	1	72	3.3
	3	69	3.3
HCNF-9	1	73	3.6
	3	73	3.4

Tensile Properties

Table 5 shows the effect of the hemicellulose content and number of WDM passes on the density, tensile strength, and elastic modulus of nanopaper sheets prepared with the different HCNFs. Even though the density was lower in the nanopaper sheets from HCNFs with higher hemicellulose content, the tensile strength and elastic modulus increased with increased hemicellulose content. In the authors' previous study (Park *et al.* 2017), the HCNF was prepared by the Wise method and WDM from Korean white pine, and the pure cellulose nanofiber (PCNF) was prepared by 17.5% NaOH treatment and WDM from the obtained holocellulose. The tensile strength and elastic modulus of the non-alkaline treated HCNF nanopaper were 155 to 178 MPa and 3.9 to 4.4 GPa, respectively, which is higher than the tensile properties of the PCNF with tensile strength of 59 to 67 MPa and elastic modulus of 1.7 to 1.9 GPa. Galland *et al.* (2015) reported an improvement in the tensile strength and elastic modulus of nanopaper with higher hemicellulose content. They explained this phenomenon in terms of the better packing effect due to hemicellulose-coated cellulose in individual HCNFs. Iwamoto *et al.* (2008) also reported that hemicellulose provides a better adhesion between cellulose nanofibrils, contributing the enhanced tensile properties to the nanopaper sheets. Molin and Teder (2002) reported that pulp paper sheets with higher hemicellulose content showed a higher stiffness and tensile strength, compared to pulp paper sheets with a lower hemicellulose content. The explanation for this was that hemicellulose on the surface of the pulp fibers adhered to the fibers in the sheets, inhibiting their deformation. Furthermore, the tensile strength and elastic modulus also improved with an increased number of WDM passes. This may have been due to the enhancement of defibrillation, *i.e.*, the decrease in the diameter of HCNF, which would increase hydrogen-bonding sites between HCNFs.

Table 5. Density, Tensile Strength, Elastic Modulus, and Specific Tensile Strength of Nanopaper Sheets Prepared from HCNFs with Different Hemicellulose Content and Number of WDM Passes

Sample Code	Number of WDM Passes	Density (g/cm^3)	Tensile Strength (MPa)	Elastic Modulus (GPa)	Specific Tensile Strength (MPa·cm^3/g)
HCNF-23	1	1.30	122	3.0	94.0
	3	1.32	129	3.1	97.3
HCNF-14	1	1.32	110	2.7	83.6
	3	1.37	124	3.0	90.2
HCNF-9	1	1.33	95	2.4	71.7
	3	1.39	109	2.7	78.4

CONCLUSIONS

1. The effects of hemicellulose content on the defibrillation efficiency of holocellulose and the properties of HCNF prepared by WDM were investigated.

2. The defibrillation efficiency of holocellulose improved with decreased hemicellulose content and increased number of WDM passes, which produced smaller fibers. The decrease of the HCNF diameter resulted in an increase of specific surface area.

3. As the hemicellulose content decreased and number of WDM passes increased, the crystallinity index of the HCNFs increased.

4. The filtration time of the HCNF suspensions and the tensile properties of the nanopaper sheets increased with increased hemicellulose content. This may have been caused by the strong water holding capacity and adhesion effect between the nanofibrils of hemicellulose.

ACKNOWLEDGMENTS

REFERENCES CITED

Abe, K., Iwamoto, S., and Yano, H. (2007). "Obtaining cellulose nanofibers with a uniform width of 15 nm from wood," *Biomacromolecules* 8(10), 3276-3278. DOI: 10.1021/bm700624p

Abraham, E., Deepa, B., Pothan, L. A., Jacob, M., Thomas, S., Cvelbar, U., and Anandjiwala, R. (2011). "Extraction of nanocellulose fibrils from lignocellulosic fibres: A novel approach," *Carbohydrate Polymers* 86(4), 1468-1475. DOI: 10.1016/j.carbpol.2011.06.034

Aulin, C., Johansson, E., Wågberg, L., and Lindström, T. (2011). "Self-organized films from cellulose I nanofibrils using the layer-by-layer technique," *Biomacromolecules* 11(4), 872-882. DOI: 10.1021/bm100075e

Chang, F., Lee, S. H., Toba, K., Nagatani, A., and Endo, T. (2012). "Bamboo nanofiber preparation by HCW and grinding treatment and its application for nanocomposite," *Wood Science and Technology* 46(1), 393-403. DOI: 10.1007/s00226-011-0416-0

Cheng, Q., Wang, S., Rials, T. G., and Lee, S. H. (2007). "Physical and mechanical properties of polyvinyl alcohol and polypropylene composite materials reinforced with fibril aggregates isolated from regenerated cellulose fibers," *Cellulose* 14(6), 593-602. DOI: 10.1007/s10570-007-9141-0

Espinosa, S. C., Kuhnt, T., Foster, E. J., and Weder, C. (2013). "Isolation of thermally stable cellulose nanocrystals by phosphoric acid hydrolysis," *Biomacromolecules* 14(4), 1223-1230. DOI: 10.1021/bm400219u

Galland, S., Berthold, F., Prakobna, K., and Berglund, L. A. (2015). "Holocellulose nanofibers of high molar mass and small diameter for high-strength nanopaper," *Biomacromolecules* 16(8), 2427-2435. DOI: 10.1021/acs.biomac.5b00678

Habibi, Y., Lucia, L. A., and Rojas, O. J. (2010). "Cellulose nanocrystals: Chemistry, self-assembly, and applications," *Chemical Reviews* 110(6), 3479-3500. DOI: 10.1021/cr900339w

Himmel, M. E., Ding, S. Y., Johnson, D. K., Adney, W. S., Nimlos, M. R., Brady, J. W.,

and Foust, T. D. (2007). "Biomass recalcitrance: Engineering plants and enzymes for biofuels production," *Science* 315(5813), 804-807. DOI: 10.1126/science.1137016

Iwamoto, S., Abe, K., and Yano, H. (2008). "The effect of hemicellulose on wood pulp nanofibrillation and nanofiber network characteristics," *Biomacromolecules* 9(3), 1022-1026. DOI: 10.1021/bm701157n

Iwamoto, S., Nakagaito, A. N., and Yano, H. (2007). "Nano-fibrillation of pulp fibers for the processing of transparent nanocomposites," *Applied Physics A* 89(2), 461-466. DOI: 10.1007/s00339-007-4175-6

Jang, J. H., Lee, S. H., Endo, T., and Kim, N. H. (2013). "Characteristics of microfibrillated cellulosic fibers and paper sheets from Korean white pine," *Wood Science and Technology* 47(5), 925-937. DOI: 10.1007/s00226-013-0543-x

Kim, B. Y., Han, S. Y., Park, C. W., Chae, H. M., and Lee, S. H. (2017). "Preparation and properties of cellulose nanofiber films with various chemical compositions impregnated by ultraviolet-curable resin," *BioResources* 12(1), 1767-1778. DOI: 10.15376/biores.12.1.1767-1778

Lee, S. H., Chang, F., Inoue, S., and Endo, T. (2010). "Increase in enzyme accessibility by generation of nanospace in cell wall supramolecular structure," *Bioresource Technology* 101(19), 7218-7223. DOI: 10.1016/j.biortech.2010.04.069

Molin, U., and Teder, A. (2002). "Importance of cellulose/hemicellulose-ratio for pulp strength," *Nordic Pulp & Paper Research Journal* 27(1), 14-19. DOI: 10.3183/NPPRJ-2002-17-01-p014-019

Monshi, A., Foroughi, M. R., and Monshi, M. R. (2012). "Modified Scherrer equation to estimate more accurately nano-crystallite size using XRD," *World Journal of Nano Science and Engineering* 2(3), 154-160. DOI: 10.4236/wjnse.2012.23020

Nobuta, K., Teramura, H., Ito, H., Hongo, C., Kawaguchi, H., Ogino, C., Kondo, A., and Nishino, T. (2016). "Characterization of cellulose nanofiber sheets from different refining processes," *Cellulose* 23(1), 403-414. DOI: 10.1007/s10570-015-0792-y

Park, C. W., Han, S. Y., Namgung, H. W., Seo, P. N., Lee, S. Y., and Lee, S. H. (2017). "Preparation and characterization of cellulose nanofibrils with varying chemical compositions," *BioResources* 12(3), 5031-5044. DOI: 10.15376/biores.12.3.5031-5044

Pejic, B. M., Kostic, M. M., Skundric, P. D., and Praskalo, J. Z. (2008). "The effects of hemicelluloses and lignin removal on water uptake behavior of hemp fibers," *Bioresource Technology* 99(15), 7152-7159. DOI: 10.1016/j.biortech.2007.12.073

Peng, Y., Gardner, D. J., Han, Y., Kiziltas, A., Cai, Z., and Tshabalala, M. A. (2013). "Influence of drying method on the materials properties of nanocellulose I: thermostability and crystallinity," *Cellulose* 20(5), 2379-2392. DOI: 10.10071s10570-013-0019-z

Prakobna, K., Galland, S., and Berglund, L. A. (2015a). "High-performance and moisture-stable cellulose-starch nanocomposites based on bioinspired core-shell nanofiber," *Biomacromolecules* 16(3), 904-912. DOI: 10.1021/bm5018194

Prakobna, K., Terenzi, C., Zhou, Q., Furó, I., and Berglund, L. A. (2015b). "Core-shell cellulose nanofibers for biocomposites-Nanostructural effects in hydrated state," *Carbohydrate Polymers* 125, 92-102. DOI: 10.1016/j.carbpol.2015.02.059

Siró, I., and Plackett, D. (2010). "Microfibrillated cellulose and new nanocomposite materials: A review," *Cellulose* 17(3), 459-494. DOI: 10.1007/s10570-010-9405-y

Segal, L., Creely, J. J., Martin, A. E., and Conrad, C. M. (1959). "An empirical method for estimating the degree of crystallinity of native cellulose using the X-ray

diffractometer," *Textile Research Journal* 29(10), 786-794. DOI:
10.1177/004051755902901003

Wan, J., Wang, Y., and Xiao, Q. (2010). "Effects of hemicellulose removal on cellulose
fiber structure characteristics of eucalyptus pulp," *Bioresource Technology* 101(12),
4577-4583. DOI: 10.1016/j.biortech.2010.01.026

Wang, Q. Q., Zhu, J. Y., Reiner, R. S., Verrill, S. P., Baxa, U., and McNeil, S. E. (2012).
"Approaching zero cellulose loss in cellulose nanocrystal (CNC) production:
Recovery and characterization of cellulosic solid residues (CSR) and CNC,"
Cellulose 19(6), 2033-2047. DOI: 10.1007/s10570-012-9765-6

Wise, L. E., Murphy, M., and Daddieco, A. A. (1946). "Chlorite holocellulose, its
fractionation and bearing on summative wood analysis and on studies on the
hemicellulose," *Technical Association Papers* 29, 210-218.

Yu, H., Qin, Z., Liang, B., Liu, N., Zhou, Z., and Chen, L. (2013). "Facile extraction of
thermally stable cellulose nanocrystals with a high yield of 93% through hydrochloric
acid hydrolysis under hydrothermal conditions," *Journal of Materials Chemistry A* 1,
3938-3944. DOI: 10.1039/c3ta01150j

Yu, Y., and Wu, H. (2011). "Effect of ball milling on the hydrolysis of microcrystalline
cellulose in hot-compressed water," *American Institute of Chemical Engineers
Journal* 57(3), 793-800. DOI: 10.1002/aic12288

Zhang, L., Tsuzuki, T., and Wang, X. (2015). "Preparation of cellulose nanofiber from
softwood pulp by ball milling," *Cellulose* 22(3), 1729-1741. DOI: 10.1007/s10570-
015-0582-6